Systems and Soft Computing 6 (2024) 200128

Contents lists available at ScienceDirect

Systems and Soft Computing

journal homepage: www.journals.elsevier.com/soft-computing-letters

Posture detection of athletes in sports based on posture solving algorithms

Huan Zhang

Arts and Sports Department, Henan College of Transportation, Zhengzhou 450000, China

ARTICLE INFO

Keywords:
Sports training
Complementary filtering algorithm
Kalman filtering algorithm
Attitude solving
Inertial navigation

ABSTRACT

With the rapid development of science and technology, the field of sports is constantly exploring and applying new technical means to improve the training effect and competitive level of athletes. Among them, the athletes' posture detection technology based on the attitude solving algorithm has been widely concerned in recent years. However, the current attitude solving algorithm has the limitation of low precision and low efficiency. Aiming at this, a new attitude solving algorithm is proposed. Firstly, the coordinate system is determined according to the theory of inertial navigation, and the attitude Angle is obtained by calculating the acceleration and magnetic induction intensity. Then the current attitude matrix is calculated according to the obtained attitude Angle. The initializing quaternion based on the attitude matrix is studied. Then, according to the advantages and defects of the three sensors, a complementary filtering algorithm is proposed for data fusion, so as to reduce the error of the final attitude solution. In order to further improve the accuracy of attitude detection, the complementary filter algorithm and double-layer Kalman filter algorithm are combined to process the data, and finally the quaternion is updated. It can be seen that the detection error of the research constructed model is only 9.94%, and its three attitude angle errors are mainly concentrated between -0.5° and 0.5° The model constructed by the research can realize high-precision posture detection, which can provide more scientific and reliable training aids for gymnastics, which has very strict requirements for movements in sports. It has positive significance for the development of sports.

1. Introduction

In the traditional sports training process, athletes' movements are usually taught by coaches based on years of teaching experience. Such a method is not scientifically accurate enough for sports that require a high level of athlete movement, such as weightlifting and artistic gymnastics [1]. Motion posture detection is a quantitative description method that identifies changes in posture in a specified area and detects the relative degree of the magnitude of the object's motion. With the continuous development of gesture detection technology, human gesture detection has been widely used in the fields of medicine, sports and civil aviation [2]. Among them, in sports, there are fewer studies on the application of posture detection technology to the training of athletes. With the development of modern technology, the requirements for the measurement accuracy and stability of posture detection have gradually become higher [3]. In the posture detection technology, MEMS inertial sensors play a pivotal role, by solving the data collected by the sensors can be obtained about the position, velocity and posture angle and other information [4]. Existing human posture detection systems generally have fewer data acquisition nodes and cannot accurately capture the whole body posture data information. This leads to the captured human body posture is not precise enough and the stability is poor [5]. There are limitations in the accuracy and efficiency of the existing attitude solving algorithms, which affect the accuracy of the detection results. This is mainly due to the noise interference of sensor data, dynamic changes during movement and the complexity of human body structure. The human posture detection system has some shortcomings in data acquisition. At present, most systems only cover part of the body nodes, and can not collect the athletes' posture information comprehensively and accurately during training. As a result, some key information may be lost in the subsequent data processing and analysis, which will affect the accuracy of attitude detection. In addition, the current athlete posture detection system often lacks intelligence and real-time. Most of them rely on manual analysis and processing of data, and lack automated and intelligent processing capabilities. In view of this, the aim of this study is to propose a more accurate and efficient attitude detection model for athletes through in-depth research on attitude algorithm. Specifically, the study will combine the inertial navigation theory, through the acceleration and magnetic induction intensity to calculate the attitude Angle, and then to find the attitude

E-mail address: huanzi207@sina.com.

https://doi.org/10.1016/j.sasc.2024.200128
Received 13 June 2024; Received in revised form 22 July 2024; Accepted 30 July 2024
Available online 31 July 2024

matrix and quaternion. At the same time, according to the advantages and defects of the sensor itself, a complementary filtering algorithm is proposed for data fusion to reduce the error of attitude solution. The motivation of the research is to solve the shortcomings of the existing athlete posture detection technology, promote the scientific and technological progress in the field of sports, and provide more advanced and scientific support for the training and competition of athletes.

The innovative contribution of this research lies in the application of the pose solving algorithm in sports training, which realizes the real-time detection of athletes' motion poses. By combining inertial navigation theory and attitude algorithm, the initial alignment of athletes' attitude is realized by quaternion method. On this basis, according to the advantages and defects of the sensor itself, a complementary filtering algorithm is proposed for data fusion, which can effectively reduce the error of attitude solution. In addition, in order to further improve the accuracy of attitude detection, the method of combining the complementary filter algorithm with the double-layer Kalman filter algorithm to process the data is studied.

The research is divided into five parts. The first part is the introduction, which introduces the research background and significance, and further puts forward the research direction. The second part is the literature review part, through the analysis and summary of domestic and foreign research status, further pointed out the shortcomings of existing research and the research direction of this research. The third part is the method introduction. A new attitude detection model is constructed by using attitude detection technology and inertial navigation technology. In this part, the techniques, methods and processes used in the model are introduced in detail. The fourth part is the experimental analysis. The performance of the research design model is verified by experiments, and the experimental results are analyzed and discussed. The fifth part is the conclusion part, which summarizes the research results and experimental results, and gives the prospect of future research.

2. Related works

With the continuous development of pose detection technology, human pose detection technology is more and more widely used in medical, sports and other fields. Wu et al. proposed a faster OpenPose model (ROpenPose) in order to solve the problem of astronauts' pose detection in space capsule under weightless environment. The model uses MobileNets instead of VGG-19 and replaces the original large convolutional kernel of the OpenPose model with three small convolutions. And a residual network is proposed to suppress the hidden problem of gradient vanishing. The experimental results show that the model greatly improves the detection efficiency of the astronauts [6]. Yang et al. proposed a fully-connected attitude detection network (FADN) in order to solve the limitation problem of 3D attitude estimation based on monocular vision. The network combines neural networks with traditional pose estimation methods. Experimental results show that the FADN has high estimation accuracy and fast operation speed [7]. Blacketer et al. In order to determine the illumination conditions that maximize the differences between the light curves of the objects caused by their attitude states. The light curves were generated by a bidirectional reflection canvas function (BRDF) applied to the shape of a collection of multi-faceted objects [8]. Park et al. proposed a low-cost MEMS inertial measurement unit attitude estimation method based on an adaptive ellipsoid for smartphones in order to improve the attitude detection accuracy. Motion acceleration and magnetic interference are considered in the adaptive logic using measurement residuals. The results show that the accuracy of this method is improved by 32% compared with the traditional attitude detection method [9]. Hsu et al. developed a variable-angle two-handle 3D system for the problem that a robotic arm cannot maintain its original optimal deployment attitude during motion, and performed real-time attitude detection to continuously correct the attitude of the robotic arm. The results showed that the system was more sensitive to orientation errors [10].

Inertial navigation technology has a wide range of applications in aerospace and other fields. Zhai et al. aim to develop a robust visually-assisted inertial navigation strategy to counteract the uncertainty that occurs during vehicle travel. Their robust strategy and algorithm are used to build a robust visually-assisted inertial navigation system by fusing a monocular camera and an inertial measurement unit. The estimation error covariance matrix and Kalman gain of different scenarios are adaptively adjusted according to the one game bet (DoA) level [11]. Shen et al. proposed a self-learning Square Root-Cubic Kalman Filter (SL-SRCKF) hybrid navigation strategy in order to improve the seamless navigation capability of the inertial navigation system in GPS denial environments. The strategy is utilized to establish the relationship between the current Kalman filter gain and the optimal estimation error, and the optimal estimation accuracy is improved by the error step. The results show that this method effectively improves the navigation capability of the system [12]. Chen et al. introduced and published the Oxford Inertial Odometer dataset (OXOD) to address the problem of lack of data and poor training accuracy of deep neural networks in motion sensing and position estimation. In addition, a new lightweight framework was proposed for more efficient inference on the edges [13]. Chen et al. proposed a feasible fusion framework for indoor localization systems based on a single technique in response to the problem of fluctuating signal strengths that lead to less reliable localization. The framework utilizes particle filtering to combine data-driven inertial navigation with Bluetooth Low Power (BLF)-based localization. Experimental results show that the fusion algorithm reduces the position error by 45.37% [14]. Jin et al. designed an improved roll isolation control system using a PI controller in order to solve the problem of roll gyroscope saturation and inertial navigation failure for rotating vehicles at large pitch angles, and verified the effectiveness of the system through experimental simulation [15].

Based on the above literature content, it can be seen that most studies focus on the application of single attitude detection technology or inertial navigation technology, but how to effectively combine the two to improve the accuracy and stability of attitude detection is still a problem to be solved. In addition, there is still room for improvement in data processing and algorithm optimization, especially in dealing with sensor data noise and errors. In view of the shortcomings of existing studies, this paper firstly introduces inertial navigation technology to obtain more accurate motion data and provide more reliable basis for attitude detection. Secondly, the attitude solving algorithm is applied to calculate and analyze the athletes' attitude changes more accurately. In addition, a data processing method combining the complementary filtering algorithm and the double-layer Kalman filtering algorithm is proposed to further reduce the error of attitude solution and improve the detection accuracy. Compared with the existing research, this study not only solves the limitation of single technology application, but also makes new progress in data processing and algorithm optimization. By combining complementary filtering algorithm and double-layer Kalman filtering algorithm, this research is expected to further improve the accuracy and stability of attitude detection, and provide more reliable technical support for medical, sports and other fields.

3. Construction of athlete attitude detection model based on inertial navigation technology and attitude settlement algorithm

Many sports have strict action norms, athletes need professional guidance in normal training, but these instructions are subjective, lack of uniformity and scientific. For this reason, the study constructed an athlete posture detection model based on posture solving algorithm and inertial navigation technology. The following is a detailed description of the technology used and the construction process of the model.

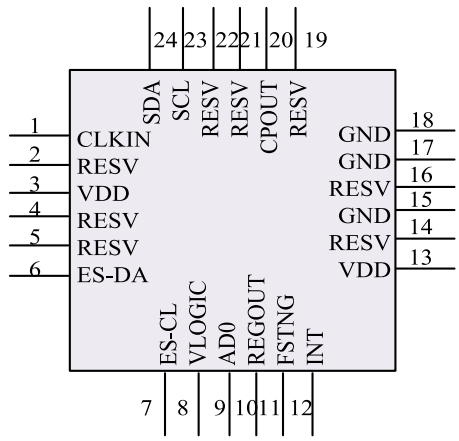

Fig. 1. Schematic diagram of MPU9150 sensor components.

3.1. Coordinate system determination and initial alignment in inertial navigation

The jetlink inertial navigation system combines inertial measurement elements such as accelerometers and gyroscopes with a carrier, where the inertial measurement elements are used to collect the sensor data, and a stable carrier platform provides the carrier for the inertial measurement eyesight and the navigation computer [16,17]. The navigation computer is used to solve the relevant data to obtain the information of position, velocity and attitude, and update them continuously. A MEMS inertial sensor is selected to complete the acquisition of basic human attitude data. According to the requirements, the MEMS inertial sensor needs to acquire three kinds of data, namely accelerated velocity, angular velocity and magnetic field strength, which is the basis for the subsequent attitude solving. The inertial sensor consists of accelerometer, gyroscope and magnetometer three sensors integrated chip. The sensor device is shown in Fig. 1.

As shown in Fig. 1, the MPU9150 sensor chip contains three components: accelerometer, gyroscope and magnetometer. The accelerometer provides motion state information for the system by measuring the acceleration data on each axis and output it after filtering. The gyroscope is responsible for measuring the angular velocity data of the MPU9150 chip around the three axes, which can reflect the change of the chip's motion attitude. The magnetometer is used to measure the magnetic field strength in the environment of the chip, so as to determine the magnetic north direction of the chip, and provide basic data for the subsequent attitude calculation. The navigation coordinate system needs to be determined first, and the determination of the coordinate system is related to the derivation of formulas in the attitude calculation [18]. The carrier coordinate system study selects the X-axis along the forward direction of the carrier, the Y-axis along the horizontal to the left direction, and the Z-axis along the vertical downward direction. The navigation coordinate system selects X, Y and Z axes along the north, east and local directions respectively. After determining the carrier coordinate system and the navigation coordinate system, the study derives them according to the Jetlink navigation principle and the attitude solution algorithm. The Euler angles are selected for the study to characterize the human body attitude. Euler angles include pitch, roll and yaw angles. The study defines the transformation order of the coordinate system, in which the transformation matrix of yaw angle rotated around the Z axis of the coordinate system is shown in Eq. (1).

$$C_1 = \begin{bmatrix} \cos\psi & \sin\psi & 0 \\ -\sin\psi & \cos\psi & 0 \\ 0 & 0 & 1 \end{bmatrix} \tag{1}$$

In Eq. (1), ψ is the yaw angle. The conversion matrix for rotating the pitch angle around the coordinate axis Y-axis is shown in Eq. (2).

$$C_2 = \begin{bmatrix} \cos\theta & 0 & -\sin\theta \\ 0 & 1 & 0 \\ \sin\theta & 0 & \cos\theta \end{bmatrix} \tag{2}$$

In Eq. (2), θ is the pitch angle. The conversion matrix for rotating the roll angle around the coordinate axis X is shown in Eq. (3).

$$C_3 = \begin{bmatrix} 1 & 0 & 0 \\ 0 & \cos\gamma & \sin\gamma \\ 0 & -\sin\gamma & \cos\gamma \end{bmatrix} \tag{3}$$

In Eq. (3), γ is the roll angle. From the transformation relationship between the carrier coordinate system and the navigation coordinate system, the attitude matrix can be obtained as shown in Eq. (4).

$$C_b^{\ n} = C_1^{\ T} C_2^{\ T} C_3^{\ T} \tag{4}$$

The interconversion between the two coordinate systems can be represented by the attitude matrix $C_b^{\ n}$, which can also be called the shortcut matrix (T). Then the attitude matrix can also be expressed as shown in Eq. (5).

$$C_b^{\ n} = T = \begin{bmatrix} T_{11} & T_{12} & T_{13} \\ T_{21} & T_{22} & T_{23} \\ T_{21} & T_{32} & T_{33} \end{bmatrix} \tag{5}$$

The comparison between the attitude angles and the elements of the attitude matrix can be obtained from the comparison of Eq. From this, the three attitude angles can be calculated. The calculation method is shown in Eq. (6).

$$\begin{cases} \gamma_T = \arctan\left(\dfrac{T_{32}}{T_{33}}\right) \\ \theta_T = \arcsin(-T_{31}) \\ \psi_T = \arctan\left(\dfrac{T_{21}}{T_{11}}\right) \end{cases} \tag{6}$$

The carrier coordinate system, the navigation coordinate system and

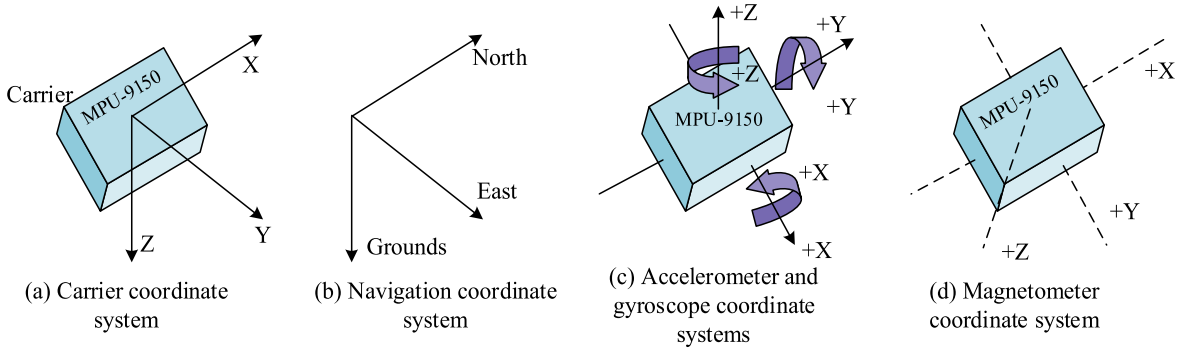

(a) Carrier coordinate system (b) Navigation coordinate system (c) Accelerometer and gyroscope coordinate systems (d) Magnetometer coordinate system

Fig. 2. Schematic diagram of each coordinate system.

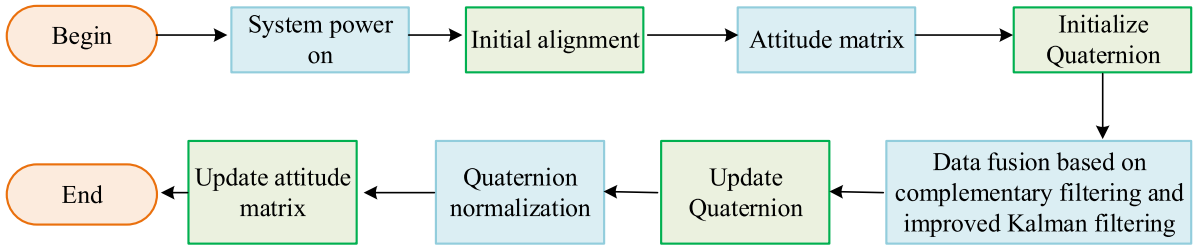

Fig. 3. Algorithm flow for solving human posture.

the coordinate system obtained by the three components are shown in Fig. 2.

The methods for solving the attitude matrix are Euler angle method, direction cosine method, and quaternion method. Synthesizing the actual situation of the research content and each solution method, the study selects the quaternion method to solve the rotation matrix. The quaternion can be regarded as a four-dimensional space, which can be expressed as shown in Eq. (7).

$$Q = q_0 + q_1 i + q_2 j + q_3 k \tag{7}$$

In Eq. (7), q_0, q_1, q_2 and q_3 are real numbers, and i, j and k are the base of the quaternion imaginary units. The computation of his human body posture needs to complete the initial alignment, i.e., to determine the initial quaternion of the system. The study solves the initial pitch, roll and yaw angles by solving the collected human body attitude data, then solves the attitude matrix and the initialized quaternion number according to the attitude matrix. The three-axis angular velocities are projected in the three axes of the carrier coordinate system. The accelerometer measurements are shown in Eq. (8).

$$f_b = \begin{bmatrix} {f_b}^x & {f_b}^y & {f_b}^z \end{bmatrix}^T \tag{8}$$

In Eq. (8), ${f_b}^x$, ${f_b}^y$ and ${f_b}^z$ are the measured values of acceleration on the three axes respectively. The projection of the gravitational acceleration on the three axes of the navigation coordinate system is shown in Eq. (9).

$$f_n = \begin{bmatrix} 0 & 0 & g \end{bmatrix}^T \tag{9}$$

In Eq. (9), g is the gravitational acceleration. Because the output of the accelerometer is not related to the yaw angle, the yaw angle in the attitude matrix is 0. At this point, the attitude matrix is brought to the accelerometer measurements to obtain Eq. (10).

$$\begin{bmatrix} 0 \\ 0 \\ g \end{bmatrix} = \begin{bmatrix} \cos\theta & \sin\gamma\sin\theta & \cos\gamma\sin\theta \\ 0 & \cos\gamma & -\sin\gamma \\ -\sin\theta & \sin\gamma\cos\theta & \cos\gamma\cos\theta \end{bmatrix} \begin{bmatrix} {f_b}^x \\ {f_b}^y \\ {f_b}^z \end{bmatrix} \tag{10}$$

The pitch and roll angles of the carrier can be calculated according to Eq. (10), as shown in Eq. (11).

$$\begin{cases} \theta = -\arcsin\left(\dfrac{{f_b}^x}{g}\right) \\ \gamma = -\arctan\left(\dfrac{{f_b}^y}{{f_b}^z}\right) \end{cases} \tag{11}$$

When the attitude angle of the carrier is not zero, according to the theoretical basis that the component of the geomagnetic field in the horizontal direction always points to the geomagnetic north pole, as well as the pitch and roll angles calculated by the accelerometer can then introduce the yaw angle formula. The measured value of the magnetometer is decomposed along the three axes of the carrier coordinate system to obtain three components, expressed as shown in Eq. (12).

$$B_b = \begin{bmatrix} {B_b}^x & {B_b}^y & {B_b}^z \end{bmatrix}^T \tag{12}$$

When the carrier coordinate system and the navigation coordinate system coincide, the components are represented as shown in Eq. (13).

$$B_n = \begin{bmatrix} {B_n}^X & {B_n}^Y & {B_n}^Z \end{bmatrix}^T \tag{13}$$

The study makes the carrier coordinate system first rotate the carrier around the Y-axis for the current pitch angle value, and then rotate around the X-axis for the current roll angle value. This in turn makes the current carrier parallel to the horizontal plane, and according to the theory of coordinate transformation can be obtained as Eq. (14).

$$\begin{bmatrix} {B_n}^X \\ {B_n}^Y \\ {B_n}^Z \end{bmatrix} = \begin{bmatrix} \cos\theta & 0 & \sin\theta \\ 0 & 1 & 0 \\ -\sin\theta & 0 & \cos\theta \end{bmatrix} \begin{bmatrix} 1 & 0 & 0 \\ 0 & \cos\gamma & -\sin\gamma \\ 0 & \sin\gamma & \cos\gamma \end{bmatrix} \begin{bmatrix} {B_b}^x \\ {B_b}^y \\ {B_b}^z \end{bmatrix} \tag{14}$$

An expression for the horizontal component of the geomagnetic field can be derived from Eq. (14), as shown in Eq. (15).

$$\begin{cases} {B_n}^X = {B_b}^x\cos\theta + {B_b}^y\sin\theta\sin\gamma + {B_b}^z\sin\theta\cos\gamma \\ {B_n}^Y = {B_b}^y\cos\gamma - {B_b}^z\sin\gamma \end{cases} \tag{15}$$

The initial yaw angle of the carrier is calculated according to Eq. (14) and Eq. (15), and the yaw angle is calculated as shown in Eq. (16).

$$\psi = \arctan\left(\frac{{B_n}^Y}{{B_n}^X}\right) \tag{16}$$

After obtaining the initial pitch, roll and yaw angles of the carrier, it is investigated to use the three angles to obtain the initialization quaternion, and the solution formula is shown in Eq. (17).

$$\begin{bmatrix} q_0 \\ q_1 \\ q_2 \\ q_3 \end{bmatrix} = \begin{bmatrix} \cos\frac{\gamma}{2}\cos\frac{\theta}{2}\cos\frac{\psi}{2} + \sin\frac{\gamma}{2}\sin\frac{\theta}{2}\sin\frac{\psi}{2} \\ \sin\frac{\gamma}{2}\cos\frac{\theta}{2}\cos\frac{\psi}{2} - \cos\frac{\gamma}{2}\sin\frac{\theta}{2}\sin\frac{\psi}{2} \\ \cos\frac{\gamma}{2}\sin\frac{\theta}{2}\cos\frac{\psi}{2} + \sin\frac{\gamma}{2}\cos\frac{\theta}{2}\sin\frac{\psi}{2} \\ \cos\frac{\gamma}{2}\cos\frac{\theta}{2}\sin\frac{\psi}{2} - \sin\frac{\gamma}{2}\sin\frac{\theta}{2}\cos\frac{\psi}{2} \end{bmatrix} \tag{17}$$

Combining the above, the study determines the navigation coordinate system and the initial alignment of the human body attitude. The flow of the human body attitude solving algorithm is shown in Fig. 3.

As shown in Fig. 3, the research first carried out initial calibration on the data collected by the three inertial sensors, and obtained the attitude Angle by solving the acceleration and magnetic induction intensity. Then the current attitude matrix is calculated according to the obtained attitude Angle. The initializing quaternion based on the attitude matrix is studied. After the initial quaternion is obtained, the gyroscope angular velocity data is corrected, and the data fusion of complementary filter is used to realize the correction process. After correction, quaternion is updated and normalized by solving quaternion differential equation. The attitude matrix is obtained by the updated quaternion, and the attitude Angle is obtained. If the system is powered off, the solution ends; otherwise, the attitude solution continues from the data fusion.

3.2. Data fusion and attitude update based on filtering algorithm

The research is based on MEMS inertial sensors to detect the human body attitude, this detection process uses accelerometers, gyroscopes

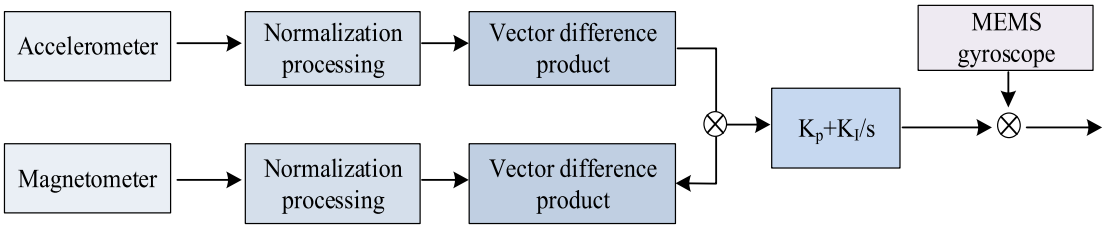

Fig. 4. Data fusion algorithm flow based on complementary filtering.

and magnetometers to collect three kinds of data: acceleration, angular velocity and magnetic induction strength, these three kinds of inertial sensors have their own characteristics. Gyroscope can provide accurate attitude information in a short time by integrating the attitude angle, but the integral calculation will make the error accumulate and there is a zero drift problem, which leads to poor long-term accuracy. Accelerometers and magnetometers do not accumulate errors over time, but have poor short-term accuracy. Based on this, the study uses a data fusion algorithm based on complementary filtering to filter and fuse the three attitude base data according to the complementary characteristics of the three inertial sensors in the frequency domain to improve the accuracy and stability of the attitude solution. When the two signals in the system are with noise, but belong to different noise, if the noise of one signal belongs to the low-frequency band, then complementary filtering can be used to filter the two signals. By this the accuracy of the signal can be enhanced. In practical applications, the accurate detection of human posture is very important for many fields. However, due to the inherent errors and limitations of various sensors, a single sensor is often difficult to meet the needs of high-precision posture detection. As an effective data fusion method, the complementary filtering algorithm can make full use of the advantages of different sensors and overcome their limitations. Through the complementary filtering algorithm, the short-term high-precision data of the gyroscope can be fused with the long-term stable data of the accelerometer and magnetometer, so as to obtain more accurate and stable attitude information. In addition, the Kalman filter can optimally estimate the sensor data according to the dynamic and noise characteristics of the system. Through the two-layer Kalman filtering algorithm, the gyroscope data and the accelerometer/magnetometer data can be filtered separately, and then fused to further reduce noise interference and error accumulation. Combining the advantages of the two filtering algorithms, this paper studies the combination of them to realize the attitude solution in static or low-speed motion scenes and dynamic and high-speed motion scenes. The study realizes data fusion based on complementary filtering. The flow of data fusion algorithm based on complementary filtering is shown in Fig. 4.

The transfer function of the complementary filter is shown in Eq. (18).

$$\begin{cases} G_1(s) = \dfrac{C(s)}{s + C(s)} \\ G_2(s) = \dfrac{s}{s + C(s)} \\ G_1(s) + G_2(s) = 1 \end{cases} \tag{18}$$

In Eq. (18), C is the input real noise-free signal, $G_1(s)$ is the characteristic with first-order low-pass filtering, and $G_2(s)$ is the characteristic with first-order high-pass filtering. The attitude information obtained by accelerometers and electronic compasses contains high-frequency noise, while the output value of MEMS gyroscopes contains low-frequency noise. Sensor 1 collects attitude information from accelerometers and magnetometers, including heading Angle, pitch Angle, and roll Angle, denoted by $C_1(s)$. The information received by sensor 2 is the attitude Angle measured by the MEMS gyroscope, which is represented by $C_2(s)$. The relationship between the real attitude information and the information obtained by the two sensors is shown in Eq. (19).

$$\begin{cases} C_1(s) = C_3(s) + \varepsilon_1(s) \\ C_2(s) = C_3(s) + \varepsilon_2(s) \end{cases} \tag{19}$$

In Eq. (19), $C_3(s)$ is the real attitude information, and $\varepsilon_1(s)$ and $\varepsilon_2(s)$ are the influence of noise on the attitude information collected by the two sensors. The collected attitude information is filtered through the complementary filter, and the attitude estimate obtained by the complementary filter is shown in Eq. (20).

$$\begin{aligned} \widehat{C}(s) &= C_1(s)G_1(s) + C_2(s)G_2(s) \\ &\approx C_3(s) \end{aligned} \tag{20}$$

The complementary filter adopts the proportional integral compensation method, and the complementary gain calculation method of the filter is shown in Eq. (21).

$$\begin{aligned} \widehat{C}(s) &= C_H(s)G_1(s) + C_L(s)G_2(s) \\ &\approx C(s) \end{aligned} \tag{21}$$

In Eq. (21), $C_H(s)$ is the high-frequency noise signal and$C_L(s)$ is the low-frequency noise signal. The complementary filter adopts the method of proportional integral compensation, and the complementary gain of the filter is calculated as shown in Eq. (21).

$$C(s) = K_p + K_I/s \tag{21a}$$

In Eq. (21), K_p is the proportional gain of the filter andK_I is the integral gain of the filter. The collected three-axis acceleration and three-axis magnetic field strength data are normalized, and after normalization, the magnetic field strength vector measured in the carrier coordinate system is converted to the magnetic field vector in the navigation coordinate system, and this vector value is the measured value of the magnetic field vector. In order to find the output error, it is necessary to find the optimal estimation of the gravitational acceleration $\widehat{v}_b$ and the estimation of the bolometric strength vector $\widehat{\omega}_b$. The calculation method is shown in Eq. (22).

$$\begin{cases} \widehat{v}_b = C_b^{\,n} \begin{bmatrix} 0 \\ 0 \\ 1 \end{bmatrix} = \begin{bmatrix} 2(q_1q_3 + q_0q_2) \\ 2(q_2q_3 - q_0q_1) \\ 1 - 2\left(q_1^{\,2} + q_2^{\,2}\right) \end{bmatrix} \\ \widehat{\omega}_b = C_b^{\,n} \begin{bmatrix} b_x \\ b_y \\ b_z \end{bmatrix} \end{cases} \tag{22}$$

In Eq. (22), b_x and b_y and b_z are the reference values of each axis of the magnetic field vector in the navigation coordinate system, respectively. The sum of the errors of each attitude angle is calculated as shown in Eq. (23).

$$e = \widehat{a}_b\widehat{v}_b \times + \widehat{m}_b\widehat{\omega}_b \tag{23}$$

In Eq. (23), $\widehat{a}_b$ and $\widehat{m}_b$ are the gravitational acceleration measured by the accelerometer and the magnetic field strength measured by the magnetometer, respectively. After calculating the sum of the errors, the study utilized it to calculate the amount of compensation for the

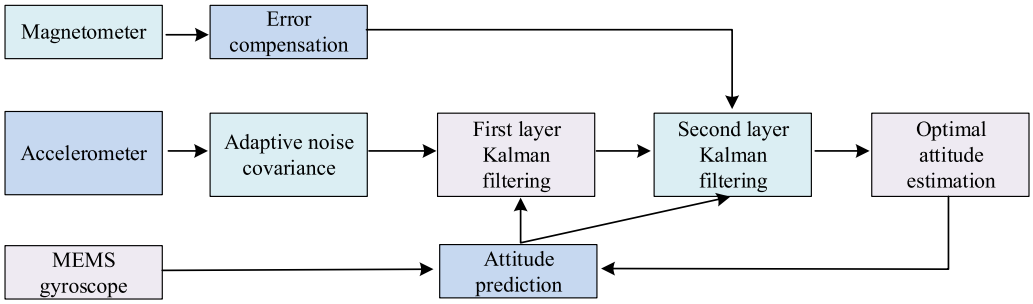

Fig. 5. Flow of data fusion algorithm based on double layer kalman filter.

gyroscope drift as shown in Eq. (24).

$$\delta = K_p e + K_I \int e \tag{24}$$

After the fusion correction of accelerometer and magnetometer, the accuracy of the gyroscope is improved. However, the cutoff frequency of the complementary filtering algorithm is not easy to determine, and there is still much room for improvement in the accuracy of solving the attitude. For this reason, the study incorporates the improved Kalman filter algorithm on the basis of the complementary filter algorithm. Considering that the accelerometer can calculate the roll angle and pitch angle independently of the magnetometer, the study proposes a two-layer Kalman filter. The flow of the dual-layer Kalman filter fusion algorithm is shown in Fig. 5.

In Fig. 5, the first layer of filtering corrects the state estimates obtained from the gyroscope by the roll and pitch angles obtained from the accelerometer, and the second layer corrects the state estimates by the yaw angle. The study utilizes complementary filters for data fusion. The final attitude angle obtained is brought to a quaternion differential equation and calculated to obtain a more accurate attitude angle. The obtained data are then input as measurements into the improved Kalman filtering algorithm for attitude solution updating. Kalman filtering is divided into two stages: prediction and update. Firstly, the predicted value of the system state is calculated, as shown in Eq. (25)

$$\overline{\widehat{q}}_k = \Phi_k \widehat{q}_{k-1} \tag{25}$$

In Eq. (25), Φ_k is the state transition matrix, $\widehat{q}_{k-1}$ is the quaternion value of the previous time, and $\overline{\widehat{q}}_k$ is the predicted value obtained from the rotation quaternion of time $k-1$. Then the predicted value of the noise covariance matrix is calculated, and the calculation process is shown in Eq. (26).

$$\overline{P}_k = \Phi_k P_{k-1} {\Phi_k}^T + Q_{k-1} \tag{26}$$

In Eq. (26), $\overline{P}_k$ is the predicted value of the noise covariance matrix, ${\Phi_k}^T$ is the transpose of the state transition matrix, Q_{k-1} is the process noise covariance matrix, and P_{k-1} is the posterior noise covariance matrix of the previous filter iteration. Then the first layer of Kalman gain is calculated and the observed error is calculated from the accelerometer measurements. Then the correction factor is calculated, and the calculation process is shown in Eq. (27).

$$q_1 = K_{k1}(Z_{k1} - h_1(\overline{\widehat{q}}_k)) \tag{27}$$

In Eq. (27), Z_{k1} is the measured value of the acceleration in the load system, K_{k1} is the first layer Kalman gain, h_1 is the carrier coordinate system after transfer, and q_1 is the correction factor. Then the updated covariance matrix is calculated, the second layer Kalman filter gain is calculated, the observed error is calculated according to the magnetometer measurement, and the correction factor updates the covariance matrix. Finally, the optimal estimate is calculated using the correction factors of the two layers. To summarize the above, the study first completed the initial alignment of the human attitude solving algorithm using the Jetlink navigation technique, and then initialized the quaternions according to the attitude matrix. In order to improve the accuracy and stability of the attitude solution, the study uses complementary filtering algorithm and double-layer Kalman filtering algorithm to construct the data fusion algorithm and realize the attitude solution. The quaternions are continuously updated according to the solving results. The attitude solving fusion algorithm based on complementary filtering and improved Kalman filtering is shown in Fig. 6.

The specific flow of the human posture detection model for the study design is shown in Fig. 7.

4. Performance analysis of athlete posture detection model based on posture solving algorithm

To test the performance of the designed model, the study designed a series of experiments to test it. In the experimental setup, the research uses high-precision gyroscopes, accelerometers, and magnetometers, which are fixed to key parts of the athlete's back and wrist to capture real-time attitude changes during movement. These sensors transmit the collected data to MATLAB environment for processing and analysis in real time through wireless transmission technology. The experimental environment includes both indoor and outdoor scenarios to test the performance of the model under different environmental conditions. A total of 200 sample sets of data from 10 athletes were collected for training and testing of the model. Before the experiment starts, the initial parameters and conditions of the model are set to ensure the correct startup and operation of the data fusion algorithm. For complementary filters, the proportional gain is set to 0.98Kp and the integral

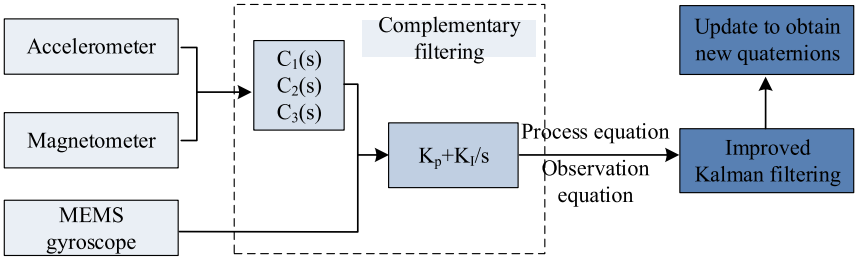

Fig. 6. Attitude calculation process based on complementary filtering and improved Kalman filtering algorithm.

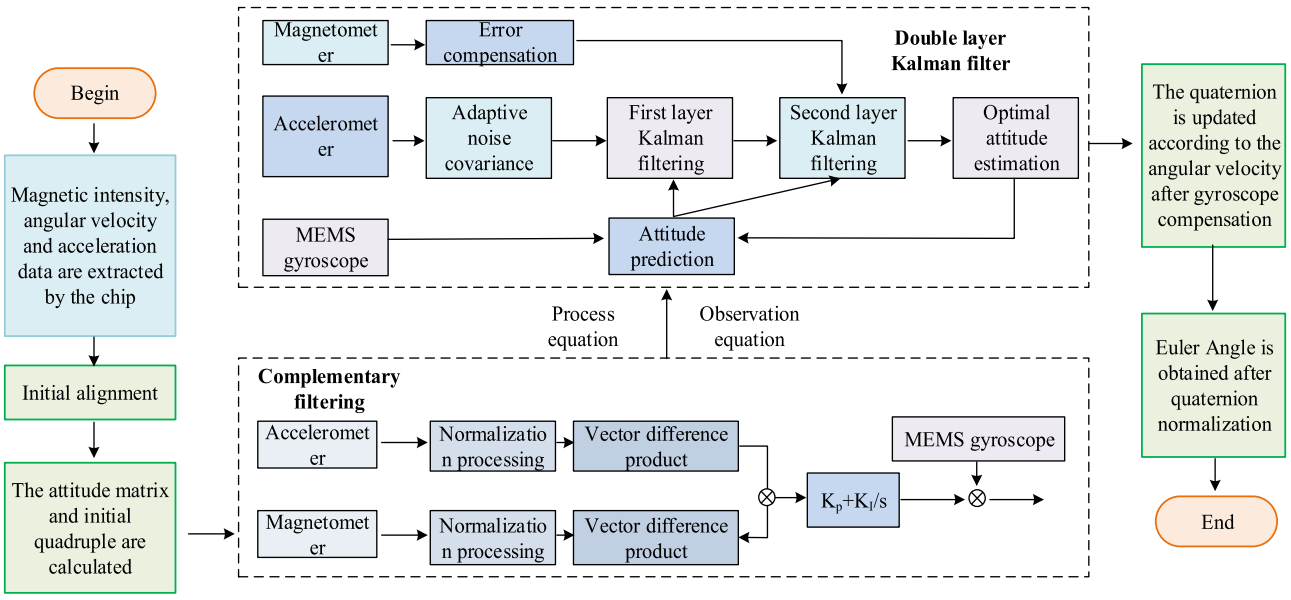

Fig. 7. The specific process of the human posture detection model.

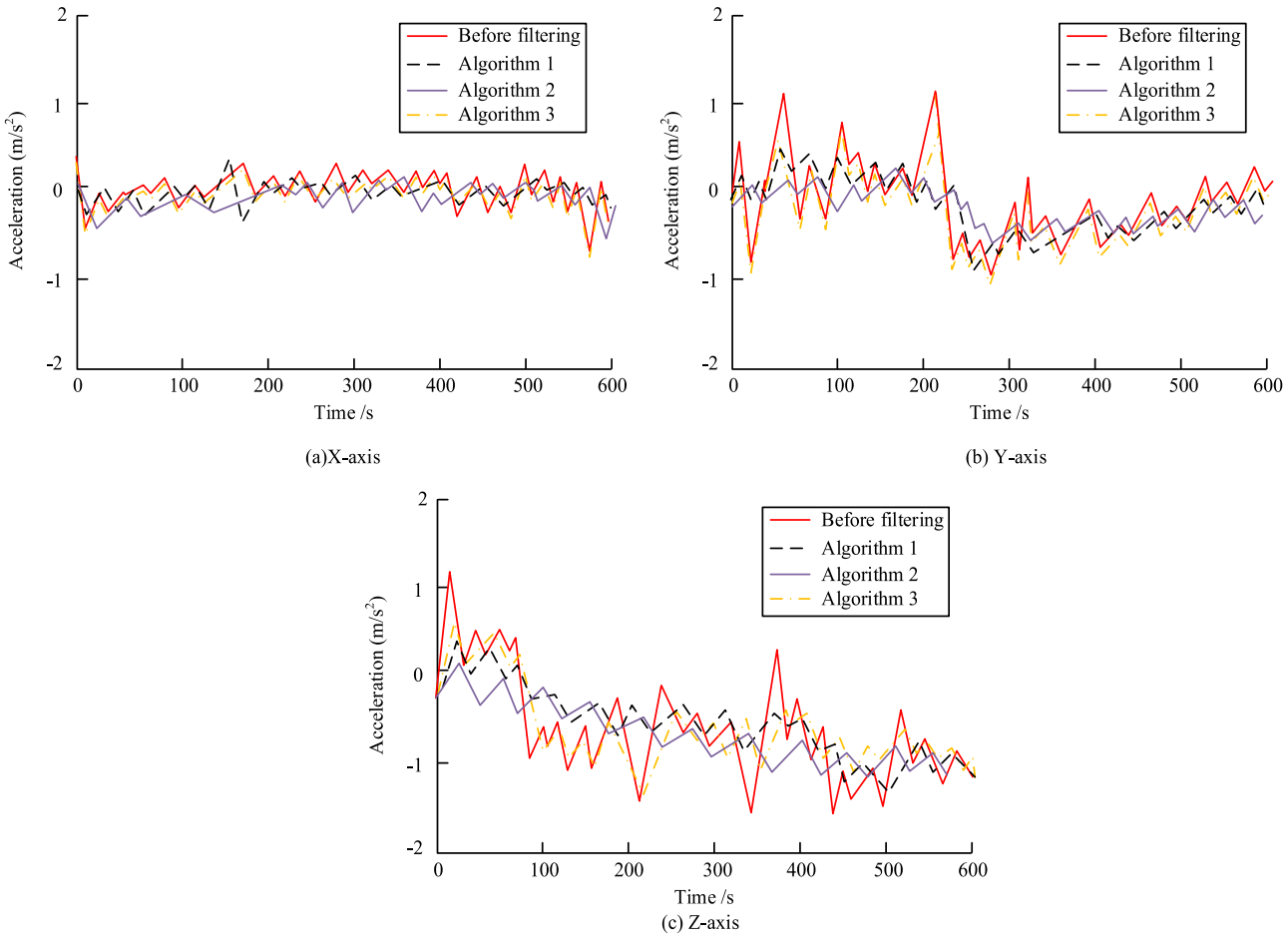

Fig. 8. Denoising results of three algorithms processing three axis acceleration data.

gain is set to 0.02Ki. For the Kalman filter algorithm, the initial estimate of the attitude Angle represented by the quaternion is set to [1,0,0,0], which represents the initial no-rotation state. The initial covariance matrix is set to [0.01, 0.01, 0.01, 0.01]. The process noise covariance matrix is set to [0.001, 0; 0, 0.001]. The measurement noise covariance matrix is set as [0.01, 0; 0, 0.01]. The sampling frequency is set to 50 Hz according to the research of sensor performance and application requirements.

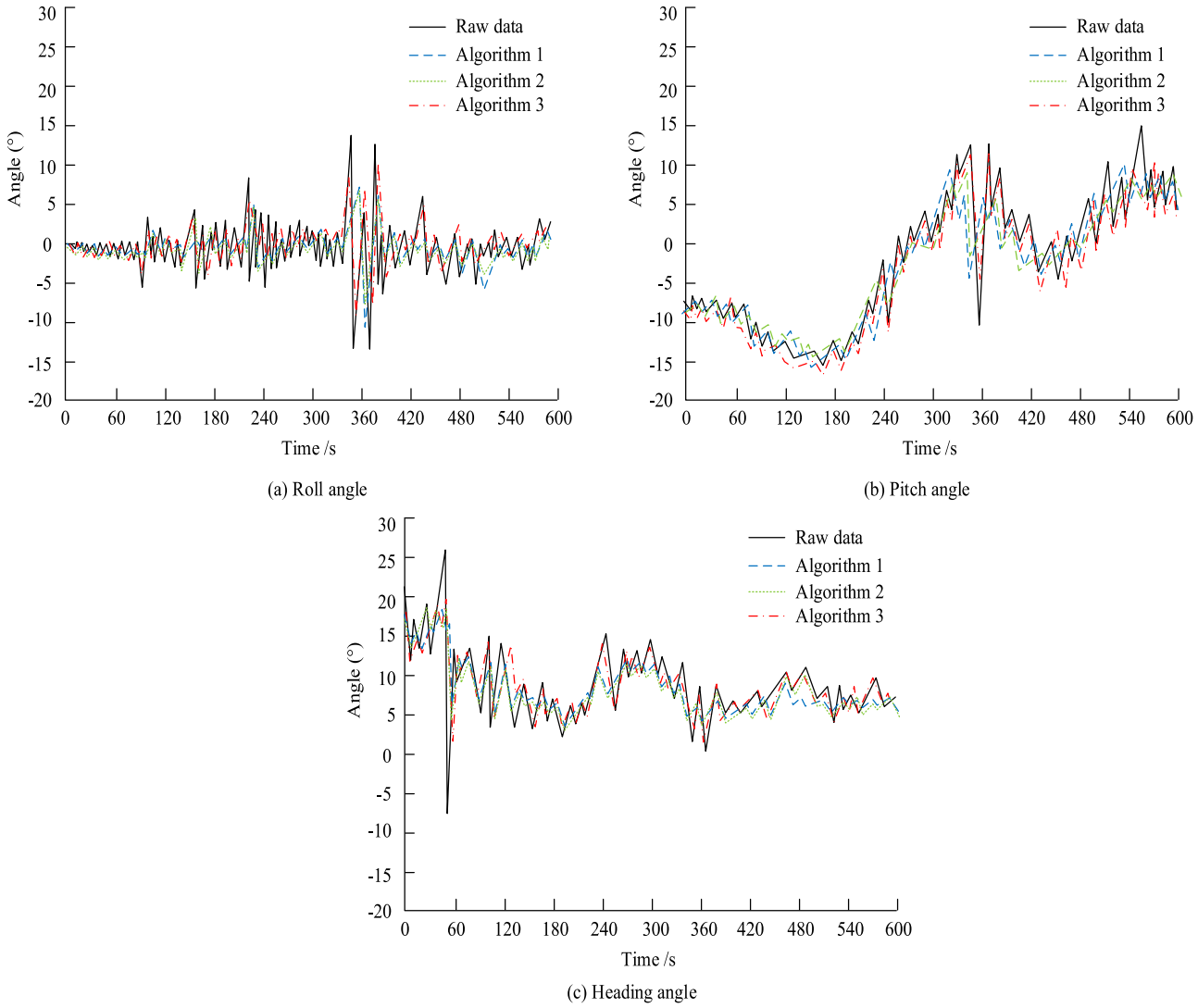

Fig. 9. Comparison of attitude angle calculation results of various algorithms.

4.1. Performance analysis of data fusion algorithm with fusion filtering

In order to improve the accuracy of attitude solution, the study uses two filter fusion algorithms to correct and fuse the attitude angle data, and finally obtains the attitude solution results. In order to check the denoising effect of the research fusion of two filtering algorithms, the experiment utilizes a single complementary filtering algorithm (Algorithm 1), an improved two-layer Kalman filtering algorithm (Algorithm 2) and a fusion filtering algorithm (Algorithm 3) to process the three-axis acceleration data, and the results are shown in Fig. 8.

As shown in Fig. 8, the fluctuation ranges of all three axes of acceleration data are significantly reduced after the filtering process. Among them, Algorithm 3 is more obvious in its effect, with better denoising effect. The curve of algorithm 3 does not change the original curve direction on the basis of the data stability is better. Comprehensive Fig. 8 shows that Algorithm 3 has a better denoising effect on the data.

In order to further verify the correctness of fusing the two filtering algorithms, the study performed attitude solving with the three algorithms. Within 10 min, the roll angle, pitch angle and heading angle are obtained using the three algorithms, and they are compared, and the

Table 1
Comparison of solution results of three algorithms for three attitude angles under different rotation angles.

Project		Error in the rotation angle of the turntable(°)						
		0	30	60	90	120	150	180
Roll angle(°)	Algorithm 1	0.62	1.02	0.99	1.08	1.51	1.50	0.68
	Algorithm 2	0.66	1.00	0.92	1.06	1.50	1.49	0.70
	Algorithm 3	0.53	0.79	0.72	0.88	1.19	1.20	0.55
Pitch angle(°)	Algorithm 1	1.88	1.40	1.33	1.54	0.51	0.69	0.81
	Algorithm 2	1.90	1.32	1.33	1.45	0.52	0.68	0.79
	Algorithm 3	1.58	1.03	1.08	1.18	0.41	0.59	0.55
Heading angle(°)	Algorithm 1	1.24	0.84	0.79	1.68	1.48	1.66	1.82
	Algorithm 2	1.01	0.80	0.65	1.52	1.31	1.38	1.59
	Algorithm 3	0.82	0.63	0.46	1.22	1.03	1.11	1.25

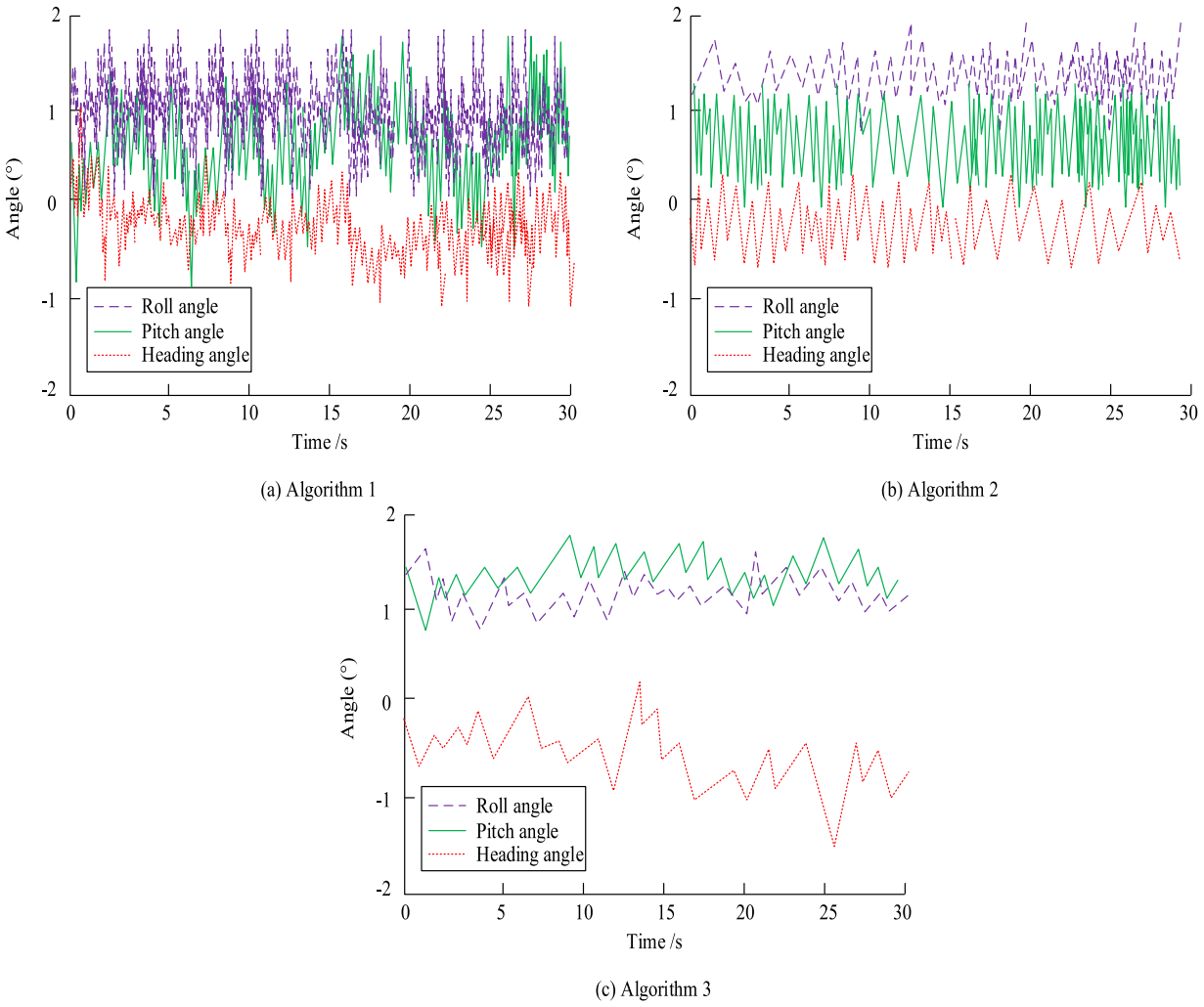

Fig. 10. Attitude calculation results of different algorithms in static state.

comparison results are shown in Fig. 9.

As shown in Fig. 9, the average errors of the three algorithms obtained in the roll angle are 1.20°, 0.96° and 0.77°, respectively; the errors in the pitch angle are 0.98°, 0.84° and 0.65°, respectively; and the errors in the yaw angle are 1.10°, 0.93° and 0.74°, respectively. Compared with the complementary filtering algorithm and the improved Kalman filtering algorithm, the proposed algorithm 3 reduces the roll angle error by 35.83% and 19.79%, the pitch angle by 33.67% and 22.62%, and the yaw angle by 32.73% and 20.43%, respectively. As can be seen in Fig. 9, a single filtering algorithm is able to achieve a high resolution accuracy, but the fusion filtering algorithm is able to obtain a more accurate attitude resolution result on this basis.

In order to test its performance more comprehensively, the study fixes the sensor node on the turntable, and tests three different angles respectively, by controlling the rotation size of the three angles, and then solves the problem using three filtering algorithms, and the solution results are shown in Table 1.

As shown in Table 1, the actual test results of the three algorithms are similar to the simulation results, and the solving error of Algorithm 2 is slightly lower than that of Algorithm 1. The results of Algorithm 1 and Algorithm 2 are similar in the solving of the two attitude angles of pitch and roll, and the solving accuracy and stability of Algorithm 2 are improved in the yaw angle. Algorithm 3 improves the accuracy of solving all three attitude angles compared to Algorithm 2. And the solving error of Algorithm 3 is decreased by 21.77% compared to Algorithm 2.

4.2. Performance analysis of attitude detection model based on inertial navigation and attitude solving algorithm

In order to test the performance of the attitude solution algorithm designed by the study, the study compares the solution results of the studied method with those of the traditional attitude solution algorithm in a stationary state. This is specifically shown in Fig. 10.

As shown in Fig. 10, the main fluctuation range of the error of Algorithm 3 is −0.8°~0.4°, while the fluctuation range of the error of Algorithm 2 is −1.2°~1.0°, and the fluctuation range of Algorithm 1 is −1.4°−1.3° Comprehensively, the contents of Fig. 10 show that Algorithm 3 is able to obtain better results compared to a single filtering algorithm, which indicates that Algorithm 3 has stronger stability.

In order to examine the performance of the posture detection model (Model 1) constructed in the study, the study conducts a comparison test between it and the more popular posture detection models in existing studies. The comparison models include: Attitude solution proposed by Borah et.al. (Model 2) [19], Saeed et.al Attitude solution method proposed by (Model 3) [20], and attitude solution method proposed by Perez-Canedo et.al. (Model 4) [21]. The experiment calculates the error between the solved attitude angle and the real value of different models respectively in the dynamic situation, and obtains the comparison results of the error of the traverse angle, pitch angle and yaw angle, which are shown in Fig. 11.

As can be seen from Fig. 11, the three attitude angle errors of Model 1 are mainly concentrated between −0.5° and 0.5°, and the errors do not

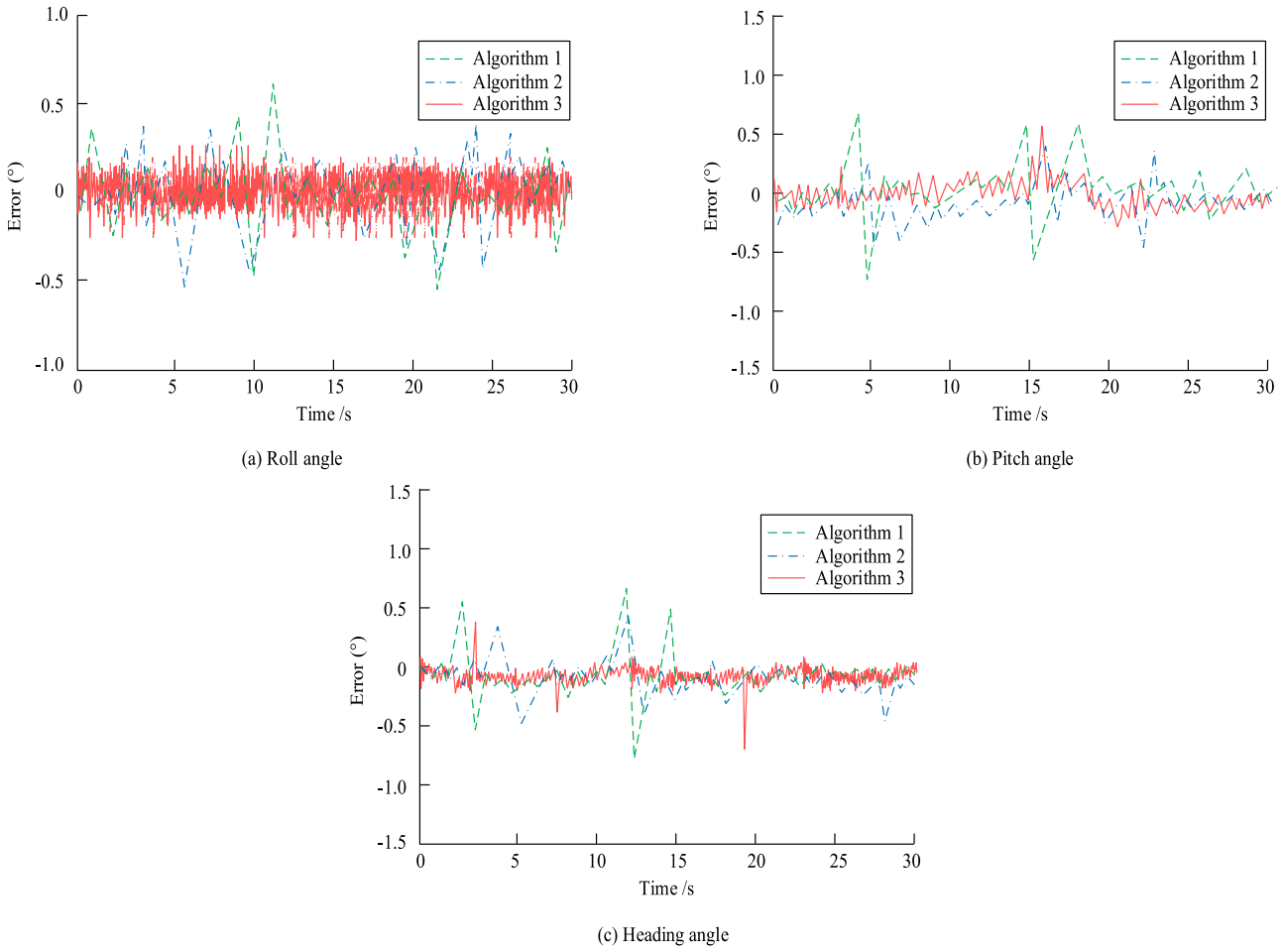

Fig. 11. Comparison of attitude calculation errors of different algorithms under dynamic conditions.

Table 2
Comparison of experimental results of measured motion postures of various models.

Project		Experiment number					
		Athlete 1		Athlete 2		Athlete 3	
		1	2	1	2	1	2
Model 1	X-axis error (%)	10.22	9.78	10.01	10.13	10.09	9.79
	Y-axis error (%)	9.79	9.55	10.05	10.23	9.90	10.02
	Z-axis error (%)	10.22	9.85	9.68	10.05	9.56	10.06
Model 2	X-axis error (%)	20.88	20.14	20.03	21.05	22.10	20.45
	Y-axis error (%)	22.11	20.84	20.11	19.78	18.44	20.45
	Z-axis error (%)	23.45	20.89	20.81	19.84	20.14	19.44
Model 3	X-axis error (%)	32.48	33.41	31.54	32.52	34.16	30.24
	Y-axis error (%)	30.45	30.21	32.45	30.54	29.45	29.98
	Z-axis error (%)	31.54	32.12	31.78	32.45	29.77	30.54
Model 4	X-axis error (%)	29.78	28.46	27.46	28.45	29.46	25.48
	Y-axis error (%)	28.46	26.88	26.89	27.48	27.66	27.18
	Z-axis error (%)	26.45	24.78	26.55	28.44	28.44	28.67

change much within 30 s of detection, basically floating within the same fluctuation range. On the other hand, the error ranges of model 2, model 3, and model 4 all fluctuate to different degrees with time. As shown in Fig. 11, model 1 can effectively suppress the problems of gyroscope output attitude dispersion and low accuracy of accelerometer and magnetometer solving. It has better dynamic performance, faster convergence speed and higher solving accuracy.

To further examine the posture detection performance of each model and its application in sports posture. The study selects three athletes to participate in the test. Their motion data were collected by MEMS inertial sensors. The experiment uses four models to detect their postures and the final detection results are recorded, as shown in Table 2.

As can be seen from Table 2, the final 3D detection error of Model 1 is 9.94%, the final 3D detection error of Model 2 is 20.61%, the 3D detection error of Model 3 is 31.42%, and the detection error of Model 4 is 27.61%. The errors of Model 1 are reduced by 10.67%, 21.48% and 17.67% respectively compared to the other three models. Comprehensive analysis of the data in the table shows that Model 1 can meet the needs of athletes' posture detection in the process of usual sports training, and can help athletes correct their movement errors in time.

In order to further compare the detection accuracy, computational complexity and anti-noise robustness of the existing attitude detection models, the detection accuracy rate and calculation time were introduced in this study, and their detection performance was recorded under three different noise interference states. The three different noise interferences are SNR =10 dB, SNR =20 dB, SNR =30 dB. The specific comparative data are shown in Table 3.

As shown in Table 3, under noise interference conditions with different SNR, model 1 is superior to the other three models in terms of

Table 3
Comparison of performance of different models under different noise interference conditions.

Noise Condition	SNR=30dB		SNR=20dB		SNR=10dB	
	Detection Accuracy (%)	Computation Time (ms)	Detection Accuracy (%)	Computation Time (ms)	Detection Accuracy (%)	Computation Time (ms)
Model 1	94.87	21.34	92.88	22.99	89.62	25.44
Model 2	82.61	33.54	80.64	36.47	79.34	38.74
Model 3	72.83	40.84	70.18	42.39	68.48	45.88
Model 4	80.32	35.88	78.94	39.15	75.44	40.31

Table 4
Ablation experiment results of key components of the model.

Component	Detection error (%)	Solution speed (ms/frame)
Original model	9.94	20.35
Without data preprocessing (A removed)	12.45	20.52
Using other inertial sensors (B replaced)	11.56	20.78
Without complementary filtering (C removed)	15.67	21.04
Without Kalman filtering (D removed)	13.44	20.86

Table 5
Statistical analysis results.

Component	Standard deviation (%)	95% confidence interval (%)	t	P
Original model	0.23	[9.71,10.17]	–	–
Without data preprocessing (A removed)	0.31	[12.14,12.76]	6.87	<0.001
Using other inertial sensors (B replaced)	0.27	[11.29,11.83]	4.21	<0.001
Without complementary filtering (C removed)	0.42	[15.25,16.09]	11.35	<0.001
Without Kalman filtering (D removed)	0.35	[13.09,13.79]	8.56	<0.001

detection accuracy. At the same time, in terms of computation time, model 1 also shows lower computational complexity, indicating that it has faster response speed and higher real-time performance in practical applications. Especially in the environment of high signal-to-noise ratio, the detection accuracy of model 1 is 96.78%, which further proves its excellent attitude detection performance.

To further verify the accuracy of the model improvement in this study, a series of ablation experiments were designed to analyze the effects of different components on the model performance. Keep other experimental conditions consistent and remove or replace key components in the model one by one to see how these changes affect model performance. Key components include data pre-processing (A), Japline inertial sensor (B), complementary filtering algorithm (C), and Kalman filtering algorithm (D). The comparison indexes include detection error and solution speed. The comparison results are shown in Table 4.

By comparing the data in Table 4, you can see the degree to which different components affect the model performance. First, when the data preprocessing component (A) was removed, the detection error went up by 2.51% and the solution speed increased slightly. This shows that data preprocessing plays a significant role in the model, which helps to reduce the noise and interference in the original data and improve the accuracy of the model. Second, the detection error also increases when it is replaced with other inertial sensors (B), indicating that Japline inertial sensor performs better in the model and can provide more accurate data. In addition, the removal of the complementary filter (C) and Kalman filter (D) results in a significant increase in the detection error and a slight decrease in the solution speed. This shows that these two filtering algorithms play an important role in the model, and they help to improve the stability and accuracy of attitude detection.

To further verify the accuracy of the model improvement and the significance of the impact of each component on the model performance, the data in Table 3 were further processed by statistical analysis. The standard deviation and 95% confidence interval were calculated for each experimental condition. Then, the T-test is used to compare whether there is a significant difference in the detection error between the original model and the model after removing or replacing the key components. The results are shown in Table 5.

As can be seen from Table 5, the mean detection error of the model after removing or replacing all key components is significantly higher than that of the original model ($P < 0.001$), and the confidence interval does not overlap with that of the original model, which further proves the accuracy of the model improvement and the significant impact of each component on the model performance. In particular, when the complementary filtering algorithm is removed, the mean detection error increases by 5.73% and the confidence interval expands significantly, which indicates that the complementary filtering algorithm plays a crucial role in improving the accuracy of attitude detection. Similarly, the removal of the Kalman filter algorithm (D) also resulted in a significant increase in detection errors, further validating its importance in stabilizing model performance.

5. Conclusion

In order to help coaches, athletes and other professionals to improve the quality of training and provide more reliable training aids, the study constructs a posture detection model for sports athletes based on inertial navigation technology and posture solving algorithm. Using the quaternion method to realize the initial solving of human posture, and then using the complementary filtering algorithm and the improved Kalman filtering algorithm to realize data fusion, correct the solving error, and finally get the estimated value of human posture. Through the experimental analysis, it can be seen that the data fusion algorithm combining the two filtering algorithms can effectively avoid the limitations of a single filtering algorithm and improve the accuracy of the solution. Compared with Algorithm 1 and Algorithm 2, Algorithm 3 reduces the roll angle error by 35.83% and 19.79%, the pitch angle by 33.67% and 22.62%, and the yaw angle by 32.73% and 20.43%. Moreover, the main fluctuation range of the error of Algorithm 3 is $-0.8^\circ \sim 0.4^\circ$, while the fluctuation range of the error of Algorithm 2 is $-1.2^\circ \sim 1.0^\circ$, and the fluctuation range of Algorithm 1 is $-1.4^\circ \sim 1.3^\circ$ It can be seen that Algorithm 1 has stronger stability. The three attitude angle errors of model 1 are mainly concentrated in the range of -0.5° to 0.5°, and within 30 s of detection, the errors do not change much, basically floating in the same fluctuation range. And the final 3D detection error of model 1 is 9.94%. Model 1 has better dynamic performance, faster convergence speed and higher solving accuracy. It can provide scientific and reliable training assistance for athletes. The current research has demonstrated the effectiveness of the proposed athlete posture detection model in improving training quality and providing reliable training assistance. However, there are still some limitations that need to be addressed in future work. The current model relies on

specific inertial sensors, which have shown good performance in experiments. However, performance may vary depending on different sensors or conditions. Therefore, future work can explore the compatibility of this model with a wider range of sensors to ensure its robustness and portability. The current model focuses on attitude detection in a controlled environment. In practical applications, athletes often face complex and unpredictable conditions such as temperature changes, vibrations, and rapid movements. Future research can investigate the robustness of models under various environmental conditions and propose adaptive or robust algorithms to mitigate the impact of external factors.

CRediT authorship contribution statement

Huan Zhang: Writing – review & editing, Writing – original draft, Visualization, Project administration, Methodology, Formal analysis, Data curation, Conceptualization.

Declaration of competing interest

The authors declare that they have no known competing financial interests or personal relationships that could have appeared to influence the work reported in this paper.

Data availability

Data will be made available on request.

References

[1] A.T. Hasanov, S.D. Akzamov, D.T Abduraimov, Pedagogical technology in professional-practical physical training of students of the faculty of military education, International Journal of Research in Commerce, It, Engineering and Social Sciences 16 (10) (2022) 148–156.
[2] J.J. Morales, Z.M Kassas, Tightly coupled inertial navigation system with signals of opportunity aiding, IEEE T Aero Elec Sys 57 (3) (2021) 1930–1948.
[3] N. Feter, R. Alt, C.A. Häfele, et al., Effect of combined physical training on cognitive function in people with epilepsy: results from a randomized controlled trial, Epilepsia 61 (8) (2020) 1649–1658.
[4] G.C. Dobre, M. Gillies, X. Pan, Immersive machine learning for social attitude detection in virtual reality narrative games, Virtual Real-London 26 (4) (2022) 1519–1538.
[5] Y. Yu, X. Zhang, M.S.A Khan, Attitude heading reference algorithm based on transformed cubature Kalman filter, Meas. Control. 53 (7-8) (2020) 1446–1453.
[6] E.Q. Wu, Z.R. Tang, P. Xiong, C.F. Wei, A. Song, L.M Zhu, ROpenPose: a rapider OpenPose model for astronaut operation attitude detection, IEEE T Ind Electron 69 (1) (2021) 1043–1052.
[7] J. Yang, M. Xi, B. Jiang, J. Man, Q. Meng, B. Li, FADN: fully connected attitude detection network based on industrial video, IEEE T Ind Inform 17 (3) (2020) 2011–2020.
[8] L. Blacketer, H. Lewis, H. Urrutxua, Identifying illumination conditions most suitable for attitude detection in light curves of simple geometries, Adv. Space Res. 69 (3) (2022) 1578–1587.
[9] S. Park, J. Park, C.G Park, Adaptive attitude estimation for low-cost MEMS IMU using ellipsoidal method, IEEE T Instrum Meas 69 (9) (2020) 7082–7091.
[10] S.C. Hsu, H.Y. Chan, T.H. Li, K.S Chen, Development of general wiimote 3D localization scheme and its application on robot arm attitude detection, Journal of the Institute of Industrial Applications Engineers 8 (1) (2020) 8–15.
[11] C. Zhai, M. Wang, Y. Yang, K Shen, Robust vision-aided inertial navigation system for protection against ego-motion uncertainty of unmanned ground vehicle, IEEE T Ind Electron 68 (12) (2020) 12462–12471.
[12] C. Shen, Y. Zhang, X. Guo, X. Chen, H. Cao, J. Tang, J. Li, J Liu, Seamless GPS/inertial navigation system based on self-learning square-root cubature Kalman filter, IEEE T Ind Electron 68 (1) (2020) 499–508.
[13] C. Chen, P. Zhao, C.X. Lu, W. Wang, A. Markham, N. Trigoni, Deep-learning-based pedestrian inertial navigation: methods, data set, and on-device inference, IEEE Internet Things 7 (5) (2020) 4431–4441.
[14] J. Chen, B. Zhou, S. Bao, S. Liu, Z. Gu, L. Li, Y. Zhao, J. Zhu, Q. Li, A data-driven inertial navigation/Bluetooth fusion algorithm for indoor localization, IEEe Sens. J. 22 (6) (2021) 5288–5301.
[15] S. Jinchao, Y. Shuxing, F. Xiong, Control failure of the roll-isolated inertial navigation system under large pitch angle, Chinese J Aeronaut 33 (10) (2020) 2707–2715.
[16] A.M. Guess, N. Malhotra, J. Pan, P. Barberá, H. Allcott, T. Brown, J.A Tucker, How do social media feed algorithms affect attitudes and behavior in an election campaign? Science (1979) 381 (6656) (2023) 398–404.
[17] M.M Gupta, Performance analysis of arl of statistical control charts for standard and modified ewma, Matrix Science Mathematic 5 (2) (2021) 42–45.
[18] J.A. Paul, M. Zhang, Decision support model for cybersecurity risk planning: a two-stage stochastic programming framework featuring firms, government, and attackers. government, and attacker, Eur J Oper Res 291 (1) (2021) 349–364.
[19] P. Borah, J. Hwang, Y.C Hsu, COVID-19 vaccination attitudes and intention: message framing and the moderating role of perceived vaccine benefits, J. Health Commun. 26 (8) (2021) 523–533.
[20] M. Saeed, M.R. Ahmad, A.U Rahman, Refined pythagorean fuzzy sets: properties, set-theoretic operations and axiomatic results, JCCE 2 (1) (2022) 10–16.
[21] B. Pérez-Canedo, J.L Verdegay, On the application of a lexicographic method to fuzzy linear programming problems, JCCE 2 (1) (2023) 47–56.